Journal of Harbin Engineering University
ISSN: 1006-7043

Vol 46 No. 12
December 2025

Optical Functions, Thermal Stability and Anti-Bacterial Assessment of 4-Chloro-N-(3,4-methylenedioxybenzyl) - aniline (CMA) Crystal

D. Preethi[1*], C. Andal[2], S. Devi[3] & E. Kavitha[4]

[1]Research Scholar, Department of Physics, Dr. M.G.R. Educational and Research Institute, Chennai-600095, Tamil Nadu, India.

[2,4]Professor, Department of Physics, Dr. M.G.R. Educational and Research Institute, Chennai-600095, Tamil Nadu, India.

[3]Research Scholar, Department of Physics, Dr. M.G.R. Educational and Research Institute, Chennai-600095, Tamil Nadu, India.

Corresponding author: preethidilli1999@gmail.com*

Abstract

A organic nonlinear optical crystal, 4-Chloro-N-(3,4-methylenedioxybenzyl)aniline (CMA), was successfully integrated and grown using the slow evaporation method. The molecular was manipulated using piperonaldehyde, 4-chloroaniline, and sodium borohydride to obtain a structurally stable, optically transparent, and suitable for crystal growth. Single X-ray diffraction confirmed that CMA crystallizes in the orthorhombic noncentrosymmetric space group $Pca2_1$. Powder X-ray diffraction patterns are used to sharp and intense reflections, confirming high crystallinity and structural order. Ultraviol visible showed two characteristic absorption edges, 282 nm and 343 nm, followed by more than 90% transmittance in the visible region. The optical band gap was determined to be 3.16 eV, indicating wide bandgap behaviour and a strong insulating nature. Dielectric analysis yielded a dielectric constant of 1.35, substantiating low dielectric loss and stable polarization response. Thermogravimetric and differential Thermal analysis (TG/DTA) analysis indicates thermal stability of the melting point of 153 °C. Antibacterial studies revealed the inhibition of the Staphylococcus aureus and Escherichia coli. The SHG efficiency of the CMA was found to be 27 % of KDP, confirming the NLO activity.

Keywords: Slow evaporation, XRD, Optical study, NLO, Antibacterial.

1. Introduction

Nonlinear optical (NLO) crystals play a purpose in modern photonics due to their aptitude to generate strange optical frequencies, modulate light, and enable ultrafast optical processes. The rudimentary motivation for growing NLO crystals lies in their capability to exhibit strong second and third-order non-linearities, which are essential for applications such as frequency doubling, optical switching, and electro-optic modulation. The laser technologies advance, there is an accelerating necessity for materials that retain high optical nonlinearity, a wide transparency window, minimal optical loss, and terrific thermal stability. These requirements necessitate the development and growth of high-quality NLO crystals with a defined non-Centro symmetric structure [1,2]. Moreover, the organic NLO crystals are exhibit faster response times and lower dielectric constants, and lower loss in certain spectral regimes compared to many inorganic counterparts [3].

In this research work, the organic 4-Chloro-N-(3,4-methylenedioxybenzyl)- aniline (CMA) crystal was grown using the slow evaporation method at room temperature. The piperonaldehyde donates an electron effectively aromatic framework and a reactive aldehyde group, enabling the formation of a stable molecular structure with strong π–π interactions. These features support the development of well-ordered crystal with desirable optical properties. 4-Chloroaniline devote a rigid aromatic amine segment dipole and structural

stability enhances intermolecular interactions. Which promotes the formation of crystals suitable for optical, dielectric, and nonlinear optical (NLO) applications. Sodium borohydride distributes as an effective reducing agent that stabilizes the reaction intermediate, yielding a thermally stable and optically transparent molecule. This stabilized product ensures good nucleation and smooth crystal growth. The grown CMA crystal was characterized using single XRD for the determination of its cell parameters and UV-visible studies for linear optical studies, including absorption and transmission studies. The SHG efficiency, confirms the nonlinear optical activity of CMA sample. Similarly dielectric constant of the grown CMA crystal is to confirm the existence of its nonlinear optical properties for photonic applications.

2. Materials and methods

The aforementioned chemical (CMA) was grown utilizing the slow evaporation method. Piperonaldehyde (1.5 g, 10 mmol) and 4-chloroaniline (1.27 g, 10 mmol) were refluxed in an ethanol solvent at room temperature for in the vicinity of 6 hours. Refluxing the amalgamation continuously for approximately two more hours followed the addition of borohydride sodium (1.52 g, 40 mmol). Along with the existing solution, 20 ml of acetone and 40 ml of water were added at this point. After the reaction combination was cooled, the resulting products were filtered. Consequently, after 30 days of growth, the result was a colourless transparent crystal and as seen in Fig.1.

Fig.1. As grown 4-Chloro-N-(3,4-methylenedioxybenzyl)-aniline (CMA) crystal

3. Results and discussions

3.1 Single XRD Analysis

It has been determined by the use of single-crystal X-ray Diffraction (XRD) analysis that the lattice parameters, the organization, and the spacing of atoms in the crystalline material have been estimated. Additionally, the internal lattice features of crystalline substances, such as the dimensions of the unit cell, bond lengths, and bond angles, are described in addition to the determination of the crystal structure.[4,5] Crystallographic data for the generated CMA crystal were obtained through single-crystal X-ray diffraction experiments. These studies were conducted with a Bruker AXS diffractometer equipped with MoKα radiation (λ = 0.7107 Å). The produced CMA crystal has an orthorhombic structure characterized by the non-centrosymmetric space group Pca21. This observation transpired as stated by the SHELX97 software, the cell traits that were measured are as follows: a = 11.133 (Å), b = 11.139 (Å), c = 21.1778 (Å), α = 90°, β = 90°, γ = 120°, V = 2624.95 (Å^3), and Z = 4. The above values are in excellent accord with the data that was presented.

3.2 Powder XRD Analysis

The powder X–ray diffraction (PXRD) pattern of the CMA sample Fig. 2, shows a series of sharp, intense, and well-defined diffraction peaks distinguished mainly between 10° and 50° (2θ). Powder Xray diffraction analysis of the synthesized compound was carried our using a Bruker D8 advance diffractometer equipped with Cu K**α radiation (λ = 1.5406 Å).** The presence of the high-intensity reflection confirms the crystalline nature of the synthesized compound. Several peaks exhibit high intensities, which suggests the presence of crystallographic aspects typically resulting from structural packing within the lattice. The compatible peak sharpness also implies a large crystalline size and supports the high quality of the grown CMA crystal. overall, the PXRD analysis confirms the CMA sample is highly crystalline, structurally ordered, and suitable for optical and solid-state applications [6].

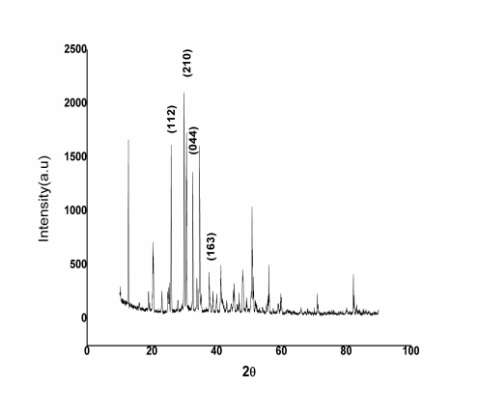

Fig.2 PXRD Pattern of grown 4-Chloro-N-(3,4-methylenedioxybenzyl)-aniline (CMA) crystal

3.3 UV –Vis Absorption

The constructed crystal's UV-Vis absorption, which is illustrated in Fig. 3, reveals obvious electronic transitions that show off the aromatic conjugated system's special features. The aromatic ring's high-frequency π → π* transition produces a significant absorption band that appears in the deep UV region (210–230 nm). At λc = 282 nm, a second, distinct peak was identified. This peak looked like the n → π* transitions that occur when there are non-bonding electrons in the substituent groups. This signal proved that functional groups were connected to the aromatic framework. In annex to these high-energy conversions, the spectrum exhibits a wide absorption shoulder at λc = 343 nm, arising from a lower-energy π → π*.Beyond this region, the material demonstrates excellent optical transparency around the visible domain, indicating a low defect concentration and high optical purity [7-9]. The UV cutoff and wide transparency window emphasizes the suitability of the crystal for nonlinear optical (NLO) and photonic applications.

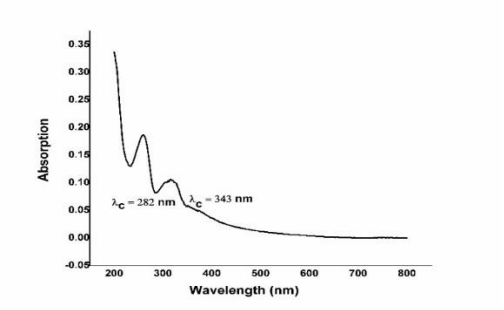

Fig.3 UV-vis absorption spectrum of the CMA sample

3.4 UV -vis Transmittance

The optical properties of the grown crystal were comprehensively analysed using optical characterisation. The UV-VIS transmittance spectrum, (Fig. 4), the Tauc plot (Fig.5) the extinction coefficient (K) interpretation with wavelength, (Fig.6), and the band gap with wavelength (Fig.7) are used to explain band gap. The UV-Vis transmission spectrum was recorded in the range of 200 – 900 nm, exhibiting two prominent absorption edges at 282 nm and 343 nm, analogous to characteristic electronic transitions within the materials. The strong absorption is observed in the deep UV region, while a sharp increase in transmittance beyond 350 nm results in more than 90% transparency in the visible region, substantiating the excellent optical clarity of the grown crystal. Which yielded an optical band value of 3.16 eV, this is in good agreement with the calculated values from the cutoff wavelength, confirming the wide bandgap of its insulating nature [10,11].

The extinction coefficient K was determined using, and its variation with wavelength is exhibited in Fig.6. The K and λ plot shows that the extinction coefficient attains its maximum near the UV absorption region and gradually increases with increasing wavelength. However, the magnitude of K remains low in the visible and near infrared regions, indicating minimal absorption loss and substantiating the high transparency of the material.

Additionally, the variation of the bandgap (E_g) with wavelength in Fig.7 confirms that the optical bandgap decreases progressively with increasing wavelength, illustrating a stable optical response and consistent electronic structure across the measured spectrum. The wide bandgap and low extinction coefficient in the visible region confirm the crystal suitability for photonic and optoelectronic applications. Overall optical analyses, including UV-Vis transmittance, absorption coefficient, Tauc plot, and extinction coefficient, show that the grown crystal exhibits excellent transparency, minimal optical loss, and strong insulating behaviour, making it a promising candidate for NLO devices, laser frequency conversion, and optical switching applications [12].

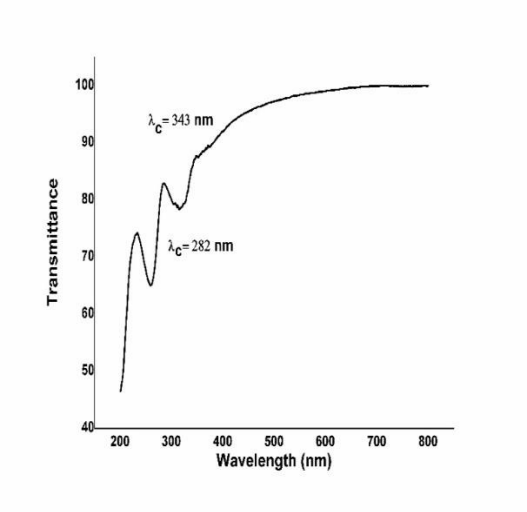

Fig.4 UV-vis transmittance spectrum of the CMA sample

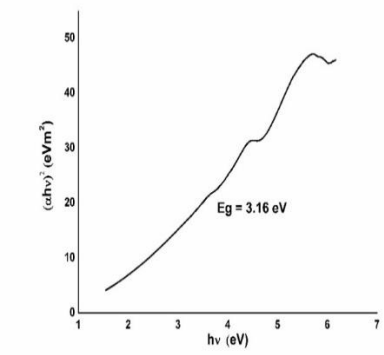

Fig.5 Tauc plot of the CMA crystal

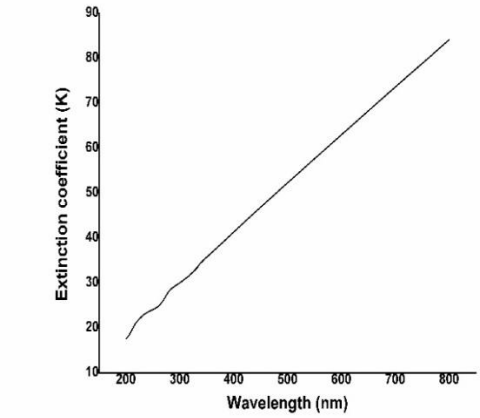

Fig.6 Variation of extinction coefficient (K) values with respect to the wavelength (λ)

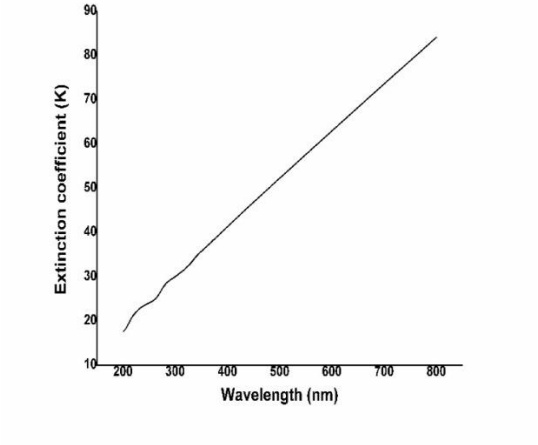

Fig.7 Variation of band gap (E_g) for the wavelength (λ)

3.5 Dielectric Constant Studies

The dielectric constant is a fundamental electrical property of crystalline materials and plays a crucial role in distinguishing phase transitions, polarization demeanor, and the suitability of a material for optoelectronic applications [13]. To decide the dielectric constant (ε_r) of the grown CMA crystal, a Dielectric constant dimension setup Fig.8 (for solid and liquid samples) was used. The investigative procedure involved weighing capacitance under the different conditions. First, the capacitance C_1 was recorded without placing any sample between the capacitor plates, serving as the reference. Next, a test material of known properties was introduced, and the corresponding capacitance C_2 was measured for calibration. Finally, the grown CMA crystal was placed between the plates, and the capacitance C_3 was attained. The dielectric constant of the CMA crystal was calculated using the standard relation,

$$\varepsilon_{r=}\frac{C_{1-}C_2}{C_{1-}C_3}$$

using the measured capacitance values, the dielectric constant of the grown CMA was found to be

$$\varepsilon_{r=1.35}$$

A dielectric constant in this range indicates the crystal possesses low dielectric s los s and stable polarization behavior, which are

desirable characteristics for optoelectronic and photonic device applications.

Fig.8 Experimental setup used for the measurement of the dielectric constant

3.6 Thermogravimetric and Differential Thermal Analyses (TG / DTA)

The thermal behaviour of the grown CMA crystal was interrogated using simultaneous TG – DTA analysis, and the corresponding TG -DTA is presented in Fig.9. The TG curve shows a gradual mass reduction beginning near 50 °C, indicating the removal of moisture and trace volatile impurities. A more continuous weight loss occurs from around 100 °C to 350 °C. The DTA curve exhibits a clear endothermic peak at 153 °C, which is attributed to the melting of the CMA crystal. Beyond this point, a broad exothermic region is observed, which is associated with the thermal degradation and breakdown of the material, comparable to the major weight loss in the TG curve. Overall, the TG -DTA results confirm that the CMA crystal is thermally stable up to its melting point (153 °C) and subsequently undergoes gradual decomposition. This level of stability indicates that the material is suitable for applications requiring moderate thermal endurance, as well as for optoelectronic components and nonlinear optical devices.

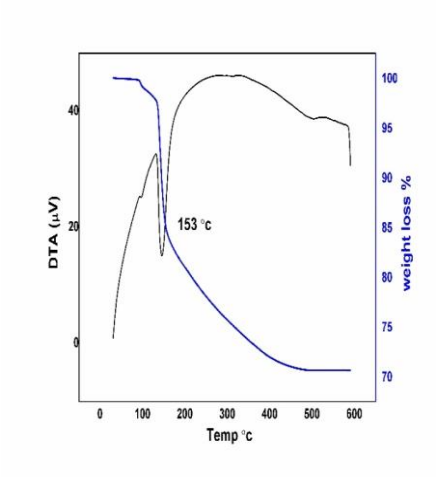

Fig.9 TG-DTA curves of CMA crystalline samples

3.7 Antibacterial Activity

The antibacterial efficacy of the synthesized CMA amalgamation was evaluated against Staphylococcus aureus and Escherichia coli, utilizing the agar well diffusion method Fig.10. Nutrient agar medium was prepared according to the standard composition and sterilized before use. The plates were inoculated with the respective bacterial cultures, and wells (8mm) were loaded with CMA at concentrations of 250,500, and 1000 µg/mL. Tetracycline was chosen as the standard reference. After incubation at 37 °C for 24h, the diameter of the inhibition zones was recorded to assess antibacterial activity. CMA exhibits stronger activity against S. aureus than E. coli. The highest restraint zones observed were 17 mm for S. aureus and 15 mm for E. coli at 1000 µg/mL (Table 1). The results indicate that CMA possesses dependent antibacterial properties, making it a potential candidate for antimicrobial coating and biomedical applications.

Table 1: Antibacterial activity of the CMA sample

S. No	Organisms	Zone of inhibition (mm)			Standard (Tetracycline)
		250 µg/mL	500 µg/mL	1000 µg/	

				mL	
1.	Staphylococcus aureus	12	15	18	15
2.	Escherichia coli	10	14	15	13

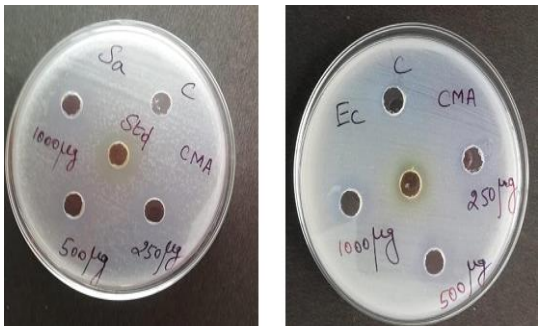

Fig.10 Antibacterial studies of CMA crystal

3.8 Nonlinear optical test

The second harmonic generation (SHG) productivity of CMA was ascertained utilising a Q-switched high-energy Nd laser (QUANTA RAY Model LAB–170–10), Model HG-4B, high efficiency, angle-tuned, and temperature-stabilized. The system utilised a second harmonic generator. The laser emits pulses with an incident wavelength of 1064 nm, which are propagated to a second harmonic wavelength of 532 nm (green light). The system performs at a repetition rate of 10 Hz with pulse duration of 6 ns; in this SHG experiment, the input energy was evaluated at 7.0 mJ for the reference KDP crystal and 1.9 mJ for the CMA sample. Compared to KDP, the SHG efficiency of CMA produces 27% of the output under identical laser input conditions which shows the required nonlinear optical properties for photoionic applications.

4. Conclusion

An organic CMA crystal was prosperous synthesized and grown with terrific structural, optical, and thermal characteristics. Single XRD verifying the CMA crystallizes in a non-centrosymmetric orthorhombic structure, which establishes the suitability of the nonlinear optical applications. PXRD results verified the high crystallinity and well-ordered nature of the grown crystal. The optical analysis revealed mighty UV absorption, wide transparency above 350 nm, and a high optical band gap of 3.16 eV, demonstrating the materials insulating behaviour and optical purity. Dielectric studies confirmed a low dielectric constant (εr = 1.35), consistent with stable polarization and reduced dielectric losses. The thermal analysis determined a good thermal stability of the melting point, 153 °C. Antibacterial tests displayed inhibition, especially against S. aureus. Then, the SHG efficiency, measured at 27 % of KDP, confirms the nonlinear optical activity of CMA. Overall, the results of the CMA crystal possesses high transparency, structural stability, wide bandgap dielectric loss, and measurable SHG efficiency, showing that the material could be used in nonlinear optical devices, laser frequency conversion, photonic components, and optoelectronic applications.

REFERENCES

[1] Richards, D., & Clays, K. (2010). *Organic nonlinear optical materials: Advances in molecular design*. Chemical Reviews, 110(1), 215–239. https://doi.org/10.1021/cr900264z.

[2] Pan, S., Xu, B., Wang, Z., & Chen, C. (2015). *Recent progress on nonlinear optical crystals*. Journal of Crystal Growth, 429, 1–11. https://doi.org/10.1016/j.jcrysgro.2015.07.024.

[3] Zheng, Y., Guan, J., Cheng, P., Han, W., Xu, J., & Bu, X.-H. (2023). *Second-order nonlinear optical organic crystals based on a "click" compound*. Journal of Materials Chemistry C, 11, 6724–6729. https://doi.org/10.1039/D3TC00652B

[4] S. Nalini Jayanthi, A. R. Prabakaran, D. Subashini, K. Thamizharasan, *Growth, optical, dielectric and fundamental properties of NLO active L-histidinium perchlorate single crystals*, International Journal of ChemTech Research, Vol. 8, No. 8, pp. 240–244, 2015. https://doi.org/10.1016/j.matpr.2015.07.062.

[5] Shu-Ping Yang, Li-Jun Han, Da-Qi Wang, Hai-Tao Xia, *4-Chloro-N-(3,4-methylenedioxybenzyl)-aniline*, Acta Crystallographica Section E, Vol.

63, p. o4403, 2007. https://doi.org/10.1107/S1600536807051732

[6] Pan, S., Xu, B., Wang, Z., & Chen, C. (2015).*Recent progress on nonlinear opticalcrystals.* Journal of Crystal Growth, 429,1-11. https://doi.org/10.1016/j.jcrysgro.2015.07.024

[7] Prasad, A.; *et al.* UV–Visible Spectral Analysis of Organic Semiconducting and Nonlinear Optical Crystals. *J. Mol. Struct.* 2018, *1160*, 224–232. DOI: 10.1016/j.molstruc.2018.01.024.

[8] Bairagi, D.; *et al.* Optical Absorption and Electronic Transitions in Aromatic Schiff-Base Crystals. *Optik* 2020, *208*, 164–171. DOI: 10.1016/j.ijleo.2019.164127.

[9] Paul, B. K.; *et al.* UV–Vis Absorption and Optical Transparency of Substituted Anilinium-Based NLO Crystals. *Mater. Chem. Phys.* 2017, *199*, 30–37. DOI: 10.1016/j.matchemphys.2017.07.056.

[10] Paavai Era, R. O. MU. Jauhar, T. Kamalesh, T. Prakash, V. Siva, *Theoretical insight on the optical centred electrical properties of guanidinium isophthalate NLO crystal for electro-optic* Q switches, Heliyon,Vol.9,Issue7,pp.1–10,ArticleID:e18311,July2023. https://doi.org/10.1016/j.heliyon.2023.e18311.

[11] Sakunthaladevi, R.; Jothi, L. *P-Chloroanilinium ethanoate: growth, characterization and NLO studies.* Journal of Minerals and Materials Characterization and Engineering 2020, *8*, 140–155. DOI: 10.4236/jmmce.2020.83009

[12] Zhang, X., Lee, J. H., & Stemmer, S. (2021). *$KTaO_3$ — The New Kid on the Spintronics Block*. Advanced Materials, 33, 2106481. https://doi.org/10.1002/adma.202106481

[13] Dessale Alemu, Shita Firehun, Tizazu Abza, M. Esthaku Peter, *The study of structural, optical, and dielectric properties of magnesium chloride-doped triglycine sulphate ferroelectric single crystals*, Advances in Materials Science and Engineering,Vol.2022, pp.1-9. Article ID: 2421382, 2022. https://doi.org/10.1155/2022/2421382